European Scientific Journal June 2013 edition vol.9, No.18 ISSN: 1857 – 7881 (Print) e - ISSN 1857- 7431

ORIENTATED FePt NANOCRYSTALS DEPOSITED ON POROUS SILICON

A. Khajehnezhad
S.A. Sebt
Physics Research Center, Science and Research Branch,
Islamic Azad University, Tehran, Iran
R.S. Dariani
Department of Physics, Alzahra University, Tehran, Iran
M. Farle
Faculty of Physics, Universität Duisburg-Essen, Duisburg, Germany
M. Akhavan
Magnet Research Laboratory (MRL), Department of Physics,
Sharif University of Technology, Tehran, Iran

Abstract

FePt nanocrystals with $L1_0$ chemical order have high magnetic anisotropy. To form the hard magnetic $L1_0$ phase as prepared fcc FePt nanocrystals need to be heated to 600°C. We demonstrate that the morphology of chemically etched porous silicon (PS) substrates and the presence of a magnetic field during the annealing process (600 °C, 1 h) affect the particle arrangement and orientation. X-ray diffraction (XRD) and field emission scanning electron microscopy (FE-SEM) show the presence of the $L1_0$ ordered FePt particles (average diameter 15 nm) uniformly distributed on the substrate. The presence of perpendicular magnetic field during annealing increases the order parameter degree of $L1_0$ FePt NPs. These effects can be investigated from variations of the XRD peaks intensity ratio. Presence of magnetic field of 20mT in the perpendicular direction to the substrate surface increases the (001) peak intensity ratio with respect to (111) peak from 0.27 to 0.58. This effect is due to the superlattice formation at (001) direction.

Keywords: FePt nanoparticles, XRD peaks intensity ratio, particle aggregation, porous silicon, superlattice

Introduction

FePt in the $L1_0$ phase has fct structure. In this structure alternating crystallographic planes of Fe and Pt are stacked along the c-axis [1]. Such ordering of each FePt nanoparticles (NPs) is obtained after annealing above 600°C [2]. The coalescence of particles during heat treatment must be prevented. At the same time the application of a perpendicular magnetic field during annealing produces crystallographically oriented particles (pancakes) with a c-axis texture out of plane in FePt thin films synthesized by sputtering method [3].

For usage as ultrahigh density magnetic recording media hard-magnetic $L1_0$ ordered FePt NPs should have uniform size and be distributed uniformly on a suitable surface [2]. Such conditions can be fulfilled by different coating methods, preventing the coalescence of NPs during annealing.

Since SiO_2 is a high-melting-temperature compound, it can be used as the substrate. By dipping the substrate into the particle dispersion, ligand exchange occurs and a strong monolayer particle assembly is formed. This approach has been employed widely to assemble nanoparticles [4]. FePt NPs tend to sink into the SiO_2 substrates during annealing, thereby coating the FePt NPs by SiO_2. This process occurs due to the reduction of the total surface energy [5]. Ordered FePt NPs arrays with areal density of 10^{12} dots/in^2, were obtained by using porous alumina templates as deposition masks [1]. The fabrication of a porous silicon (PS) matrix has the advantage of low costs and fewer process steps. Furthermore, a silicon-based system is appropriate for integration in a microelectronic process technology [6,7].

Here, we suggest to use PS as a substrate for annealing of FePt NPs. Key parameters determining the morphology of the porous silicon layer during anodization are the electrolyte type [7], HF concentration of the electrolyte [7,8], doping type and its level in the silicon substrate [7,9,10], and current density [8,10]. In this work, FePt NPs have been produced by polyol method, and Si wafers have been anodized to produce PS wafers. Then, FePt NPs were deposited on these substrates by wet chemistry method by controlling the hexane evaporation rate and then annealed up to 600°C. Moreover, the effect of magnetic field during annealing process has been studied by the XRD and VSM analysis,

Method

The 2.22nm FePt NPs have been synthesized by the polyol method and analysed by TEM analysis which has been shown in Ref. [11]. The synthesis process of the NPs involves the reduction of iron(III) acetylacetonates and platinum(II) acetylacetonates in phenyl ether solvent in the presence of N_2 flow with the rate of 4cc/s. The 1,2 – hexadecanediol was used as the reducing agent, and oleic acid and oleylamine were used as

ligands. The contents was heated to 247°C at a rate of approximately 7°C/min, followed by refluxing at 247°C for 30 minutes before cooling down to room temperature. Afterwards, NPs solution was purified by cyclic precipitation and redispersion with ethanol and hexane and centrifugation of the NPs solvents. The smallest concentration of FePt NPs in the final colloidal hexane solution with oleic acid and oleylamine ligands was 2.5 mg/ml. One fourth of this concentration was used for samples.

To produce a suitable substrate for NPs, the porous silicon is fabricated electrochemically in the electrolyte of HF (48%): H_2O: C_2H_5OH with the ratio of 2:2:1. Anodization was performed at a current density of 50 mA/cm^2, $100mA/cm^2$, and 300 mA/cm^2 for 240s which produce pores with 20-50nm diameter. Before anodization, the backside of the P type silicon wafer with <0.005 Ω-cm resistivity was coated by a 2 μm thick Al layer for ohmic contact by evaporation (0.4Å/sec) in 4×10^{-5} mbar pressure.

The PS was immersed in the colloidal FePt hexane solution, and after vaporizing the hexane with the rate of 0.5cc/h, the FePt NPs were deposited on it. The particles on the wafer were annealed to 600°C in the presence of 90% Ar + 10% H_2 flow with the rate of 4cc/s for 1h, and then cooled to room temperature. The films were also annealed under a magnetic field of 20mT applied parallel or perpendicular to the substrate.

AFM studies were carried out using SPM Park Scientific Instruments Auto probe CP model on contact mode. Conventional SEM studies were carried out using a FE-SEM S-4160 HITACHI model at 15 kV. X-ray diffraction (XRD) studies were done by a STOE STADI MP model with the wave length of 1.54Å, voltage of 40kV, current of 30mA, step size of 0.01, and step time of 1s. The magnetic properties of the samples were investigated using a vibrating sample magnetometer, VSM, Lake-Shore model 7400 with the maximum field up to 20kOe. The structure and surface distribution were analyzed by XRD, AFM, and FE-SEM. VSM analyses show the magnetic properties.

Results And Discussions

The SEM images of FePt NPs deposited on substrates are shown in Fig. 1. In Figs. 1a and 1b the FePt NPs have been deposited on normal wafers. The sample which is shown in Fig. 1a has been annealed in the absence of magnetic field but for Fig. 1b a magnetic field has been applied perpendicular to the surface. It is shown that the absence of magnetic field causes the NPs to coalescence. A possible reason is that at high temperatures the NPs have higher random mobility which is reduced when a magnetic field is applied. One might interpret that the magnetic field applied perpendicular to the surface, causes the NPs to separate even at high temperatures, which could be related to the weak repulsive force between the magnetic dipoles which are oriented perpendicular to the surface.

Comparing the $L1_0$ FePt NPs in Figs. 1c, and 1d, reveals the effect of different current densities 50mA/cm^2 and 100mA/cm^2 on the morphology of PS. Figures 1c and 1d correspond to Figs. 2a and 2b, respectively. In Fig. 1c we can see that at 600°C, NPs coalesced clusters are produced, because the surface roughness of the wafer anodized with 100mA/cm^2 has not been suitable. Conditions for the sample in Fig. 1e are the same as for the sample in Fig. 1c, except for the application of magnetic field in the film plane in Fig. 1e during annealing.

The preparation conditions of the sample in Fig. 1f, which was annealed in the perpendicular magnetic field, are the same as the sample in Fig. 1d except for the presence of magnetic field. Comparing these two figures shows that the effect of PS on separation of FePt NPs in absence of magnetic field is more pronounced than in presence of magnetic field. Comparing Figs. 1b and 1f, reveals that the effect of the magnetic field on separation of FePt NPs on a normal wafer is more pronounced than on PS. Therefore, the effect of magnetic field and PS substrate on separating and orientation of $L1_0$ FePt NPs is maximum when they exist separately (Figs. 1b, 1d).

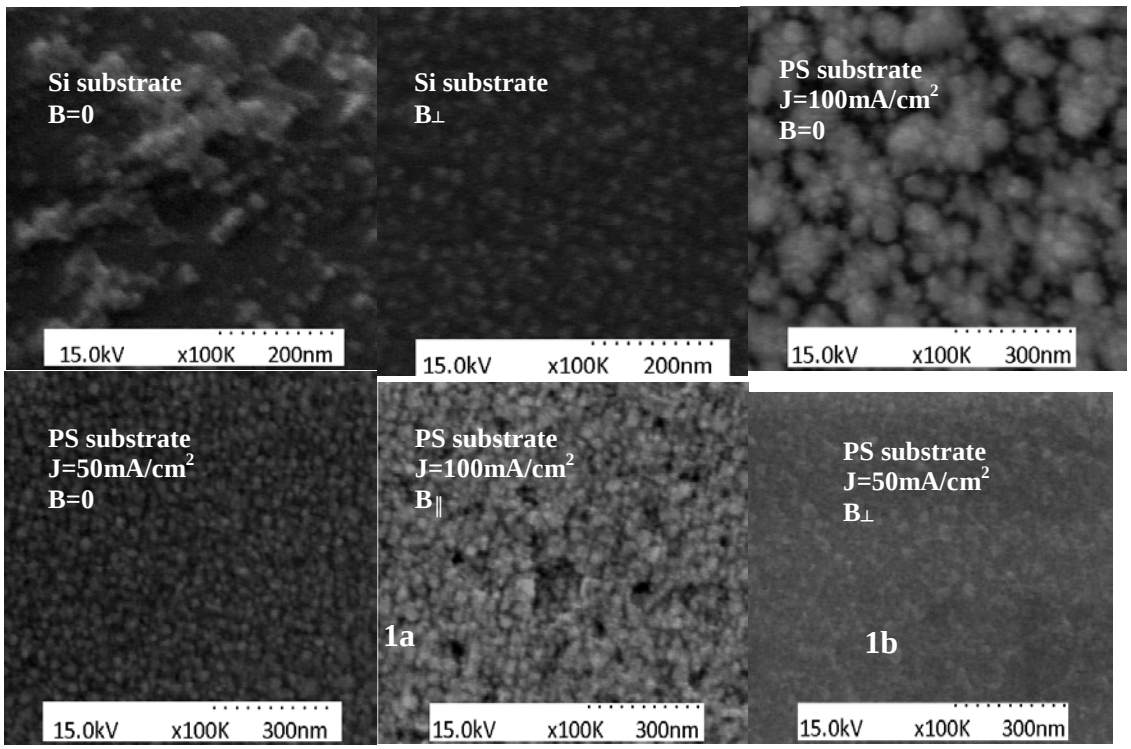

Figure 1. SEM images of deposited $L1_0$ FePt NPs on 1a) normal wafer; 1b) normal wafer in perpendicular magnetic field; 1c) PS with J=100mA/cm^2; 1d) PS with J=50mA/cm^2; 1e) PS with J=100mA/cm^2 in parallel magnetic field; 1f) PS with J=50mA/cm^2 in perpendicular magnetic field. Figs. 1b and 1d show the best samples.

Figure 2 shows AFM analyses of two wafers which are anodized in 240s in HF acid (48%): H_2O: C_2H_5OH solution that were fabricated with different current densities. On these wafers, silicon functionalizes and has dangling bonds which were produced by HF [12] and are useful for maintaining FePt NPs. Figure 2b with J=50mA/cm^2 is suitable for our work because in SEM analysis it can be seen that FePt nanoparticles are distributed more uniformly on this substrate than in the other one (compare Fig. 1c and 1d).

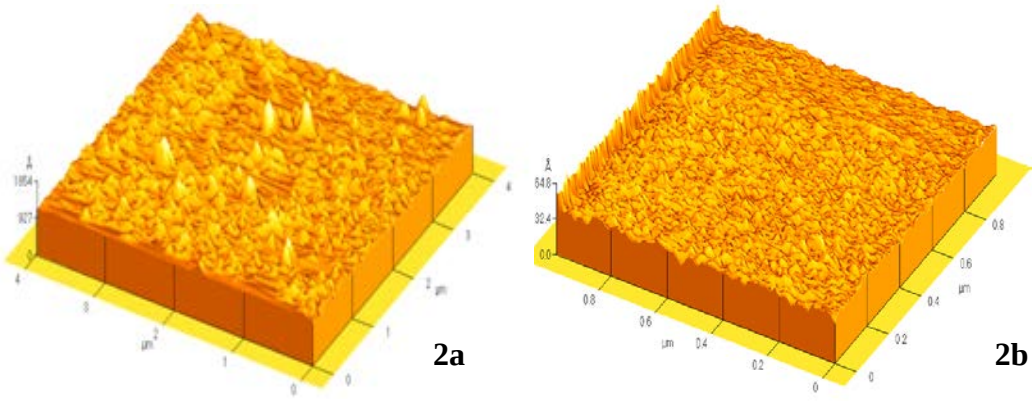

Figure 2. AFM images of porous silicon, 2a) J=100mA/cm^2, 2b) J=50mA/cm^2.

Figure 3a shows the XRD patterns of FePt NPs before annealing and figures 3b, 3c, and 3d show the XRD patterns of FePt NPs after annealing in the absence of magnetic field, and in the presence of parallel and perpendicular magnetic fields respectively. The shift of (111) peak to larger angles and also the separation of the (200) and (002) peaks in every annealed sample indicates that the c/a ratio decreased from 1 (cubic) in the crystal structure. It means that the crystal lattice structure converted from fcc to fct. Moreover, for every annealed sample, the (001), (110), and (201) peaks appeared and the $L1_0$ phase with chemical order occurred. In fact, for a single element material in fcc structure, the structure factor for these peaks is equal to zero. So, these peaks do not appear. But, for an alloy such as FePt, due to the difference in the atomic form factor for its atoms, these peaks in the $L1_0$ phase with chemical order appear.

Comparison of the width of the (111) peaks of the as prepared (Fig.3a) and annealed samples shows the dramatic increase of the particle size (from 2.22 to 15 nm), since the peaks become much sharper. By comparing figs. 3c and 3d which correspond to samples in Figs. 1e and 1b respectively, it can be seen that in perpendicular magnetic field (B⊥) NPs are better separated from each other, so the (111) peak is wider in Fig. 3d than in

Fig. 3c, but as is seen in 1e, parallel magnetic field ($B_{\parallel}$) causes NPs to coalese.

The presence of a magnetic field during annealing causes the easy axis ordering of NPs. The c axis alignment of NPs can be estimated from variations of the XRD peaks intensity ratios ($I(h_1k_1l_1)/I(h_2k_2l_2)$) [3, 13]. The I(001)/I(111) in Figs. 3b, 3c, and 3d for B=0, parallel, and perpendicular magnetic field are 0.24, 0.27, and 0.58, respectively. Therefore, it can be shown that the magnetic field causes the particles to orient themselves. It means that the easy axis of NPs is aligned in the field direction. In fact, such ordering is superlattice formation in (001) or c-axis direction. Since the orientation of nanocrystals align to (001) direction is more than for (111), the ratio I(001)/I(111) becomes larger.

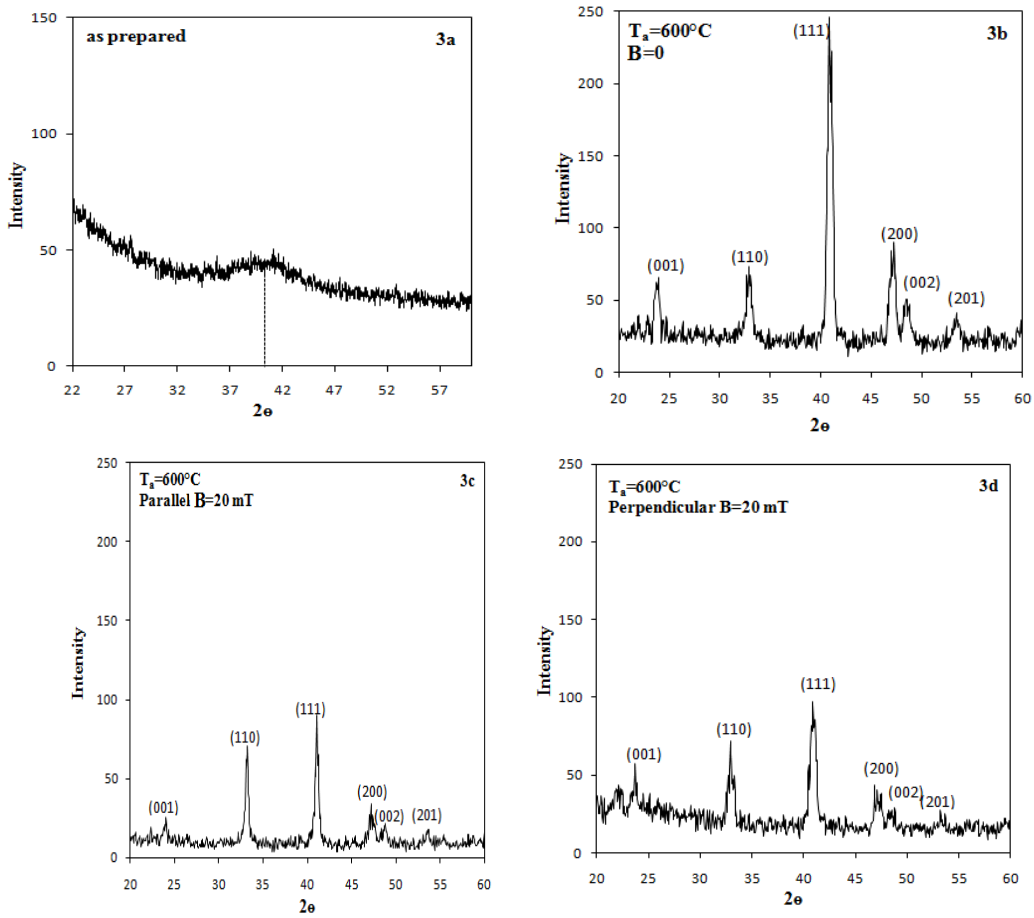

Figure 3. XRD patterns, as prepared sample 3a, and annealed sample in 600 °C in absence of magnetic field 3b, parallel magnetic field 3c, and perpendicular magnetic field 3d

Moreover, $(I(001)/I(002))^{1/2}$ is proportional to the degree of chemical order of $L1_0$ FePt phase [14,15,16]. This chemical order parameter (S) can be defined by S = rPt + rFe – 1 expression, where rPt(Fe) is the fraction of Pt(Fe) sites occupied by the correct atom [17,18]. I(001)/I(002) in Figs. 3b, 3c, and 3d, respectively, for B=0, parallel, and perpendicular magnetic field are 1.11, 1.03, and 2.16. Therefore, perpendicular magnetic field increases the order parameter degree of FePt NPs.

The magnetic analysis of two samples is shown in Fig. 4. These hysteresis loops (a and b) correspond to Fig. 1a and 1b which are annealed in the absence and presence of magnetic field, respectively. For both samples, the magnetization was measured at room temperature and in perpendicular direction to the substrate (out-of-plane). In curve b this applied field is parallel to the field which had been applied to the sample during annealing which causes NPs to orient. So, the magnetization and slope increasing in Fig. 4b with respect to Fig. 4a is due to the relative orientation of sample in the presence of magnetic field during annealing.

Furthermore, as is seen in the SEM analysis, NPs are 15nm, and also are separated from each other in Fig. 1b. Therefore, its coercivity (loop b) is lower than the other one.

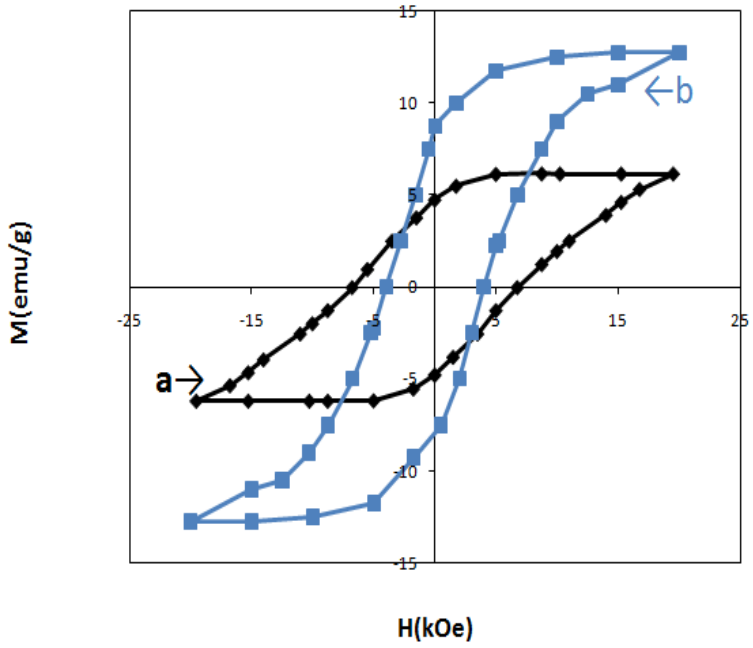

Figure 4. Magnetic hysteresis of the samples annealed in a) absence, and b) presence of magnetic field.

Conclusion

$L1_0$ ordered FePt NPs (15 nm) have been fabricated with the chemical method in order to access to oriented and uniform NCs surface distributions in $L1_0$ magnetic phase by annealing 2.22nm sized colloidal fcc FePt nanoparticles deposited on a porous silicon substrate. Annealing in a perpendicular (parallel) magnetic field with respect to the surface of the sample causes the easy axis of the magnetization (c-axis) to rotate out-of-plane (in-plane) and the NPs to separate.

The XRD peaks intensity ratios (I(001)/I(111)) increase in the presence of magnetic field. This is the evidence for increasing the orientation degree of nanoparticles in the c-axis direction. This is in addition to the internal chemical ordering of each nanoparticle, which increases in magnetic field.

References:

1. C. Kim, T. Loedding, S. Jang, and H. Zeng, *Appl. Phys. Lett.* 91, 172508 (2007).
2. S. Sun, Adv Matter 18, 393 (2006).
3. Y.B. Li, Y.F. Lou, L.R. Zhang, B. Ma, J.M. Bai, and F.L. Wei, *Journal of Magnetism and Magnetic Materials* 322, 3789 (2010).
4. M.L. Plumer, J. Van EK, and D. Weller, *The Physics of Ultra-High-Density Magnetic Recording, Berlin: Springer,* 2001, pp. 257.
5. Y. C. Wu, L. W. Wang, and C. H. Lai, *Appl. Phys. Lett.* 93, 242501 (2008).
6. S. A. Gusev, N. Korotkova, D. Rozenstein, and A. Fraerman, *J. Appl. Phys.* 76, 6671 (1994).
7. H. Föll, M. Christophersen, J. Carstensen, and G. Hasse, *Mater. Sci. Eng. R* 39, 93 (2002).
8. V. Lehmann, *J. Electrochem. Soc.* 140, 2836 (1993).
9. M. J. J. Theunissen, *J. Electrochem. Soc.* 119, 351 (1972).
10. V. Lehmann, R. Stengl, and A. Luigart, *Mater. Sci. Eng. B* 69–70, 11 (2000).
11. S. A. Sebt, A. Khajehnezhad, R. S. Dariani, M. Akhavan, J Inorg Organomet Polym, published online in 2013, DOI: 10.1007/S10904-013-9862-5
12. A. Mari, E. Agostinelli, D. Fiorani, A. Flamini, S. Laureti, D. Peddis, A.M. Testa, G. Vararo, M.V Mansilla, A. Mezzii, S. Kaciulis, Superlattices and Micro Structures, 46, 95 (2009).
13. Z.Y. Pan, J.J. Lin, T. Zhan, S. Karamat, T.L. Tan, P. Lee, S.V. Springham, R.V. Ramanujan, R.S. Rawat, *Thin Solid Films* 517, 2753 (2009).

14. S. Okamoto, N. Kikuchi, O. Kitakami, T. Miyazaki, Y. Shimada, K. Fukamichi, *Phys. Rev., B, Condens. Matter Mater. Phys.* 66 024413 (2002).
15. J. A. Christodoulides, P. Farber, M. Daniil, H. Okumura, G. C. Hadjipanayis, V. Skumryev, A. Simopoulos, and D. Weller, *IEEE Trans. Magn.*37, 1292 (2001)
16. L. Zhang, Y. K. Takahashi, A. Perumal, and K. Hono, *Journal of Magnetism and Magnetic Materials* 322, 2658 (2010).
17. J. Lyubina, O. Gutfleisch, R. Skomski, K.-H. Müller, and L. Schultz, *Scripta Materialia* 53, 469 (2005).
18. O. Gutfleisch, J. Lyubina, K.-H. Müller and L. Schultz, *Advanced Engeneering Materials* 7, *208 (2005).*